Author accepted manuscript -

Increased copy number couples the evolution of plasmid horizontal transmission and plasmid-encoded antibiotic resistance.

Tatiana Dimitriu[1*], Andrew Matthews[1], Angus Buckling[1]

[1] *Department of Biosciences, University of Exeter, Penryn Campus, Cornwall TR10 9FE, UK*

* Corresponding author: tatianadimitriu1@gmail.com

The research data supporting this publication are openly available from the University of Exeter's institutional repository at:

https://ore.exeter.ac.uk/repository/handle/10871/126437.

Title:

Increased copy number couples the evolution of plasmid horizontal transmission and plasmid-encoded antibiotic resistance.

Authors:

Tatiana Dimitriu[1*], Andrew Matthews[1], Angus Buckling[1]

[1] *Department of Biosciences, University of Exeter, Penryn Campus, Cornwall TR10 9FE, UK*

* Corresponding author: tatianadimitriu1@gmail.com

Classification:

Biological Sciences / Evolution

Keywords:

Plasmid copy number; conjugative plasmids; antibiotic resistance; plasmid transfer

Abstract:

Conjugative plasmids are mobile elements which spread horizontally between bacterial hosts, and often confer adaptive phenotypes, including antimicrobial resistance (AMR). Theory suggests that opportunities for horizontal transmission favour plasmids with higher transfer rates, whereas selection for plasmid carriage favour less mobile plasmids. However, little is known about the mechanisms leading to variation in transmission rates in natural plasmids or the resultant effects on their bacterial host. We investigated the evolution of AMR plasmids confronted with different immigration rates of susceptible hosts. Plasmid RP4 did not evolve in response to the manipulations, but plasmid R1 rapidly evolved up to 1000-fold increased transfer rates in the presence of susceptible hosts. Most evolved plasmids also conferred on their hosts the ability to grow at high concentrations of antibiotics. This was because plasmids evolved greater copy numbers, as a function of mutations in the *copA* gene controlling plasmid replication, causing both higher transfer rates and AMR. Reciprocally, plasmids with increased conjugation rates also evolved when selecting for high levels of AMR, despite the absence of susceptible hosts. Such correlated selection between plasmid transfer and AMR could increase the spread of AMR within populations and communities.

Significance statement:

Antimicrobial resistance (AMR) is typically caused by genes present on plasmids: genetic parasites that can rapidly spread between bacterial cells. We demonstrate that plasmids can evolve increased transmission when hosts are abundant by increasing the number of plasmid molecules present within cells. A side-effect of having more plasmids in a cell is a greater degree of cellular AMR. Selection for higher cellular levels of AMR in turn resulted in increased transmission via the same mechanism. Opportunities for plasmid transmission thus promote the evolution of plasmids that are both highly infectious and confer high levels of AMR on their hosts.

Main text:

Conjugative plasmids are mobile genetic elements that transmit horizontally within and between species of bacteria [1]. Plasmids often confer adaptive traits such as new metabolic abilities, virulence and antimicrobial resistance (AMR), therefore an understanding of variation in plasmid transmission rate (transfer)[2] is critical [3,4]. While greater transfer is expected to directly increase the frequency of plasmids in a population, it might also affect the phenotypes conferred by plasmids in other ways. Greater transfer may confer a cost to the host [5] (limiting growth and reducing the frequency of plasmid-carried traits), directly or indirectly modify the expression of other plasmid-encoded traits[6], or promote loss of accessory genes [7]. Finally, plasmids that are at high frequencies within communities may rapidly adapt to ameliorate their costs [8], further increasing their frequency [9–11]. Here, we experimentally investigate the consequences of selection for increased plasmid transfer rates on plasmid-encoded AMR.

Increased plasmid transfer (or parasite transmission in general) is predicted to only be favoured when susceptible hosts are present in abundance[12]. This is because the cost to host bacteria limits plasmid vertical transmission, leading to a trade-off between horizontal and vertical transmission [5]. Indeed, evolution experiments in conditions with low opportunity for transfer observe decreased transfer rates and carriage costs [10,13–15], but horizontal transmission can increase when susceptible hosts are available [5,16–18]. We evolved conjugative plasmids under variable host availability and followed the evolution of transfer rates and AMR. We used two plasmids, R1 and RP4, which have variable transfer rates in closely related host strains [19], suggesting the potential for rapid evolution. R1 and RP4 are both conjugative multidrug-resistant plasmids, but differ in replication mechanisms, host range and transfer regulation [20,21].

Results

R1 plasmid evolves high transfer rates in the presence of susceptible hosts

To vary the importance of horizontal transmission in plasmid life cycle without enforcing direct selection for plasmid-bearing cells, we passaged an initial culture of plasmid-bearing cells (either plasmid RP4 or R1) with regular influx of various proportions of immigrant plasmid-free cells, and in the absence of any antibiotic selection (Figure 1A). We used both wild-type (wt) and mutator (mut) *Escherichia coli* host; the latter to increase genetic variation available for selection. Plasmid maintenance in immigration treatments required horizontal transmission, or they would be rapidly diluted out, with plasmids in high immigration treatments

experiencing higher selection for horizontal transmission (Figure S1). RP4 plasmid was rapidly lost from all treatments with ≥ 90% immigration per day, but stably maintained over 30 days, after an initial decline, under 68% immigration. R1 plasmid was maintained for longer than RP4, but R1-bearing cell density decreased steadily for all immigration treatments, with a faster decrease under higher immigration (Figure 1B).

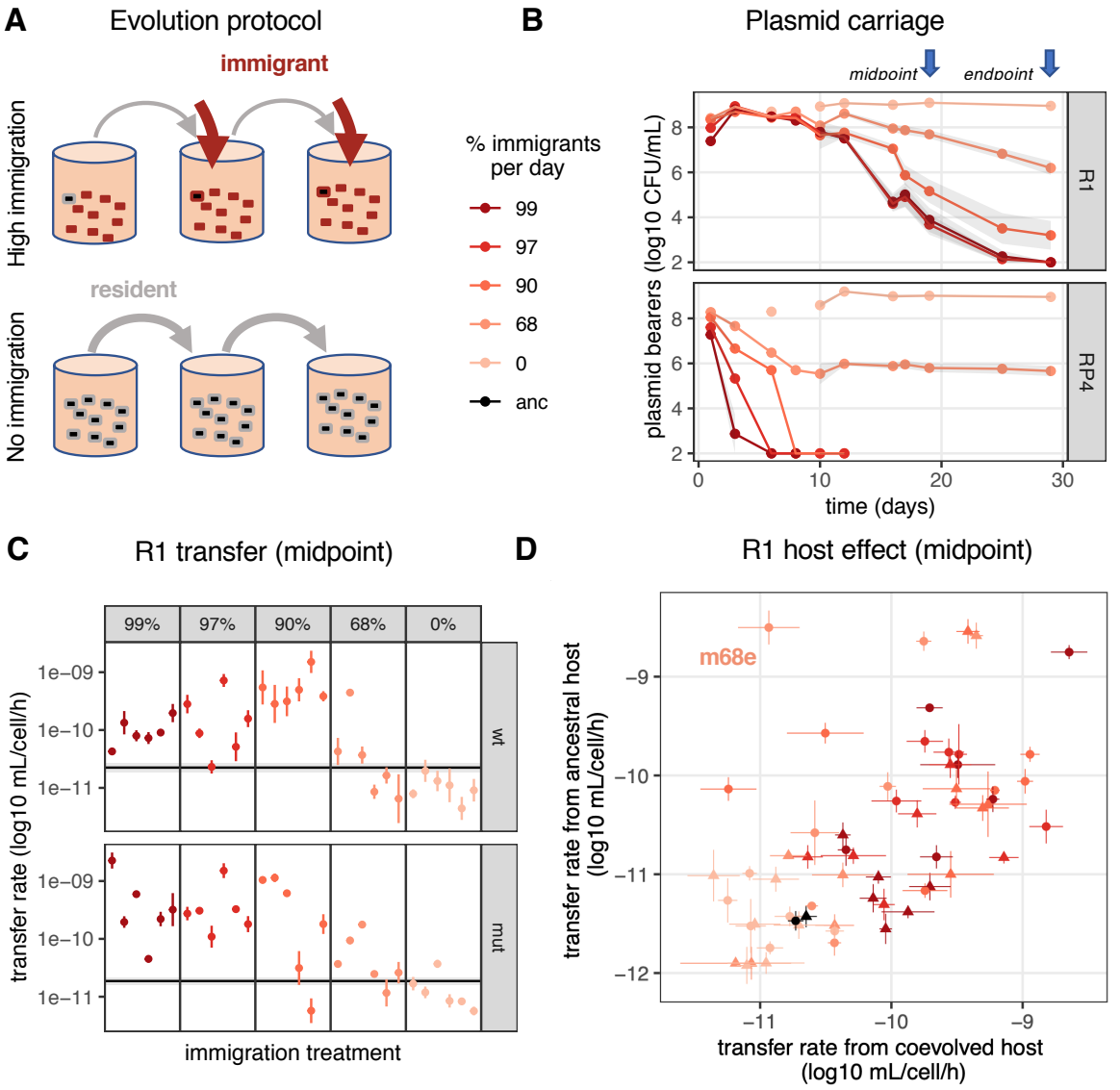

Figure 1: Evolution of plasmid transfer rate with varying host availability. A) Experimental evolution regime. Plasmid-bearing cells (black) were first mixed with plasmid-free cells, then evolving populations were diluted every day to fresh medium (grey arrows) mixed in varying frequencies to plasmid-free cells (red arrows). Each treatment was performed in 6 replicates with either wt or mut *E. coli* hosts. B) Plasmid population dynamics. Initially one of six replicates was measured until day 12; then the treatment average is shown ± s.e.m.

(shaded area). C) Midpoint R1 conjugation rates. The black line and shaded area are respectively the geometric mean and standard error (SE) of ancestral plasmid transfer rate; each coloured dot and line indicates respectively the geometric mean and SE of evolved clones (N=3). Wt clones are shown on the top, and mut clones on the bottom. D) Effect of host evolution on R1 conjugation. The x axis shows transfer rates measured from plasmid-bearing coevolved hosts (same as 1C); the y axis from ancestral hosts carrying evolved plasmids. Dots and lines indicate respectively the geometric mean and SE (N=3). Circles show the wt background and triangles the mut background.

We first measured transfer rates from coevolved plasmid-host clones to ancestral recipients. We detected no significant changes in endpoint (29 days) conjugation rates for RP4, but increased transfer for R1 with 68% immigration (Figure S2, R1 transfer rate ~ immigration, $F_{2,86}$=5.2, p=0.007). For R1, we next focused on midpoint clones, before plasmid lineages under high immigration went extinct. We observed significant effects of immigration treatment on evolved transfer rates (Figure 1C, transfer rate ~ immigration, $F_{5,198}$=43.1, $p<2.10^{-16}$). Specifically, treatments with ≥90% immigration had significantly increased transfer rates compared to the ancestor and ≤68% immigration treatments (Tukey test, $p < 2.10^{-5}$) but were not significantly different from each other (see Supplementary Text for detailed statistics and host effect). Thus, high transfer rates evolved in the presence of abundant plasmid-free recipients.

To tease out effects of host evolution on evolved transfer rates, we also measured transfer rates of midpoint evolved plasmids from the ancestral host. Transfer rates were still greater in immigration treatments (Figure S3A). Transfer rates from coevolved hosts correlated with transfer rates from ancestral hosts (Figure 1D, bivariate model Cov(coevolved, ancestral)=0.39±0.10, clone covariance effect χ=23, p=1.5.10^{-6}; correlation coefficient=0.60±0.09). Thus, increased transfer rates are mostly due to genetic changes in plasmids rather than hosts. However, a few clones diverged from this pattern, most significantly clone mut68e with a 1000-fold increase in transfer rate when the plasmid was present in an ancestral host, but not in its coevolved host (Figure 1D). This suggests that some hosts evolved repression of plasmid transfer, potentially because of transfer costs to the host.

R1 evolves higher costs

As a proxy for plasmid cost, we measured the densities reached by donor hosts during conjugation assays. Donor density was negatively correlated with transfer rates (Figure 2A, donor density ~ transfer rate, estimate=-0.53±0.03, r^2=0.56, p<2.2 10^{-16}). Host density still correlated with transfer rates when plasmids were carried by the same, ancestral host (Figure S3B), confirming that some of the reduction in cell growth is due to plasmid evolution. This trade-off likely limits the fitness benefit of increased transfer rate, by limiting plasmid vertical transmission.

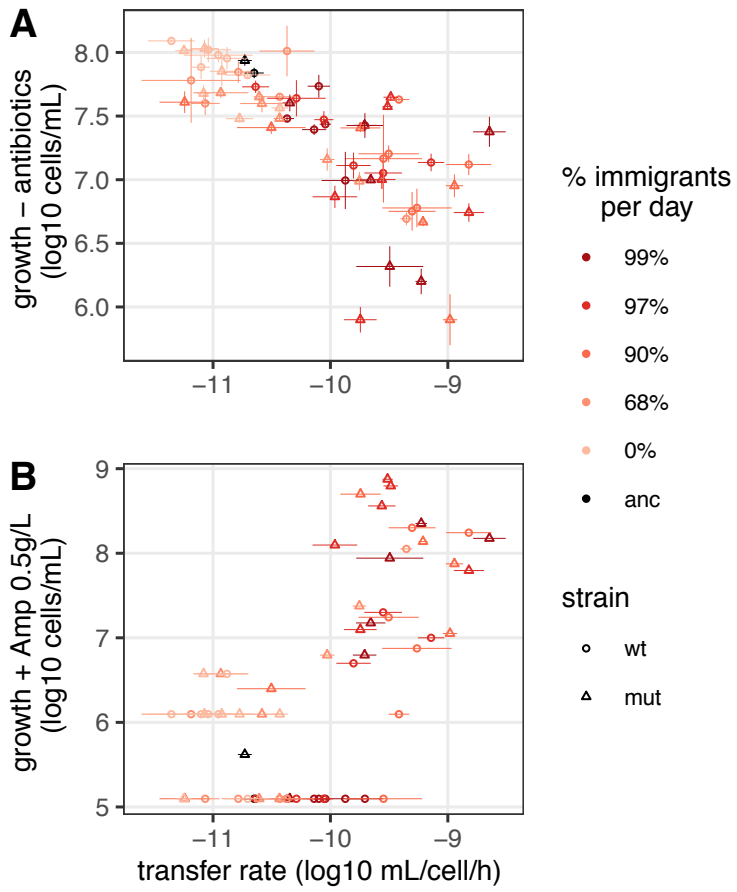

Figure 2: **Breakdown of the trade-off between transfer and host fitness under antibiotic selection**. Host growth in the absence of antibiotics (A, donor cell density during conjugation assays) and in the presence of high levels of antibiotics (B, density of cells able to grow on Amp 0.5g/L) is shown for midpoint coevolved clones as a function of their transfer rate. Dots and lines indicate respectively the geometric average and standard error (N=3).

R1 also evolves increased AMR

To evaluate if the benefits conferred by plasmids in the presence of antibiotics also evolved, we measured cell growth in the presence of high levels of antibiotics (Figure 2B). Many evolved clones conferred on their hosts an ability to grow in conditions in which the ancestor could not (Figure 2B). Most of these also had increased transfer rate (Spearman rank-correlation $\rho = 0.62$, $p = 10^{-7}$), suggesting that increased AMR is a side-effect of selection for transfer.

This apparent coupling between transmission and AMR prompted us to address if selection for high transmission co-selects increased AMR, and vice versa. First, we plated early populations from the evolution experiment directly on Amp 0.5g/L (Figure 3A). Highly resistant cells were more common in immigration treatments, especially in the mutator host ($\log_{10}$ cell density ~immigration * host, $F_{1,56}=12.8$, $p=0.0007$). In some lineages, nearly all plasmids conferred upon their hosts ability to grow at high antibiotic concentrations, and showed increased transfer compared to $R1_{wt}$ (Figure S4). Thus, immigration treatments selecting for increased transfer collaterally promote the appearance of high AMR.

Next, we determined if selection for elevated AMR also increases transfer rates in the absence of direct selection for transmission. We plated independent cultures of the ancestral host carrying $R1_{wt}$ on high levels of antibiotics, and measured plasmid transfer rate for highly resistant mutants (Figure 3B). Selection for AMR increased transfer rate overall ($\log_{10}$ transfer rate ~ selection, $F_{1,70}=30.6$, $p=5.10^{-7}$), and 13 of 18 mutants displayed increased transfer compared to $R1_{wt}$, with approximately 10-fold higher transfer rates (Figure 3B).

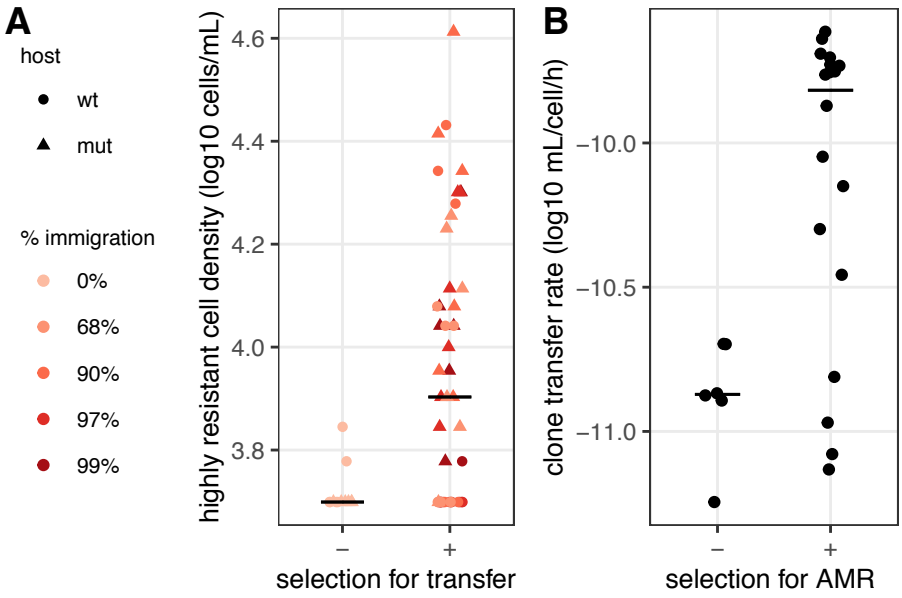

Figure 3: Reciprocal selection for high transfer rate and AMR. A: Host availability promotes the evolution of highly antibiotic-resistant plasmids. The density of cells able to grow in the presence of 0.5g/L Amp is shown for populations evolved for 9 days with or without immigration. B: Selecting for high level antibiotic resistance promotes evolution of highly transmissible plasmids. 6 independent populations of a $R1_{wt}$ clone were plated with or without high concentrations of antibiotics, and the transfer rate of 3 mutants per population measured (geometric average of N=3 replicates per mutant). Horizontal lines show the median value for each treatment.

The presence of susceptible hosts favours R1 copy-number variants

To understand the genetic basis of the evolved phenotypic changes, we sequenced midpoint evolved clones. The summary of mutations is shown in Dataset S1. Plasmid mutations were found almost exclusively in clones from immigration treatments (Figure 4A). We focus next on loci with parallel mutations in independently evolved lineages, a sign of convergent molecular evolution (but see Supplementary Text for other mutations). First, four evolved plasmids from the 90% immigration treatment contain large deletions (~10 to 20 kb), which include one or several antibiotic resistance determinants (Figure S5). Rapid loss of resistance genes by R1 was observed previously [7,14], and is likely underestimated here as we used Amp resistance as a proxy for plasmid carriage. Next, four evolved plasmids carried the same 1bp insertion in the coding region of *finO*, the main repressor of the transfer operon [20], and another carried a 7bp insertion, causing a frameshift. These mutations are known to cause loss of function and derepression of the transfer operon [22]. 17 variants had a G deletion and one a GG deletion in a polyG tract ~ 50bp before the coding region of *gene32*, part of the leading region first transferred to recipient cells. *gene32* function is unknown but it is conserved and likely important for conjugative transfer [23]. Finally, the most common mutations were in the *copA* locus. The untranslated antisense CopA RNA plays a central role in R1 replication and copy number control by inhibiting translation of the initiator for plasmid replication RepA [24]. We observed overall 27 point mutations variants contained in a 13bp region within *copA*: 9 different types of mutations were observed, but all from C or G nucleotides towards A or T, denoted as *copA** below (Figure 4A). These mutations structurally alter the head of CopA RNA's loop II that is involved in binding to RepA mRNA [24]. Identical or similar mutations were shown to increase R1 plasmid copy number (PCN) by decreasing CopA binding to RepA mRNA [25]. Accordingly, we observed increased sequencing coverage for *copA** plasmids consistent with increased PCN (Figure 4B top, detail in Figure S5).

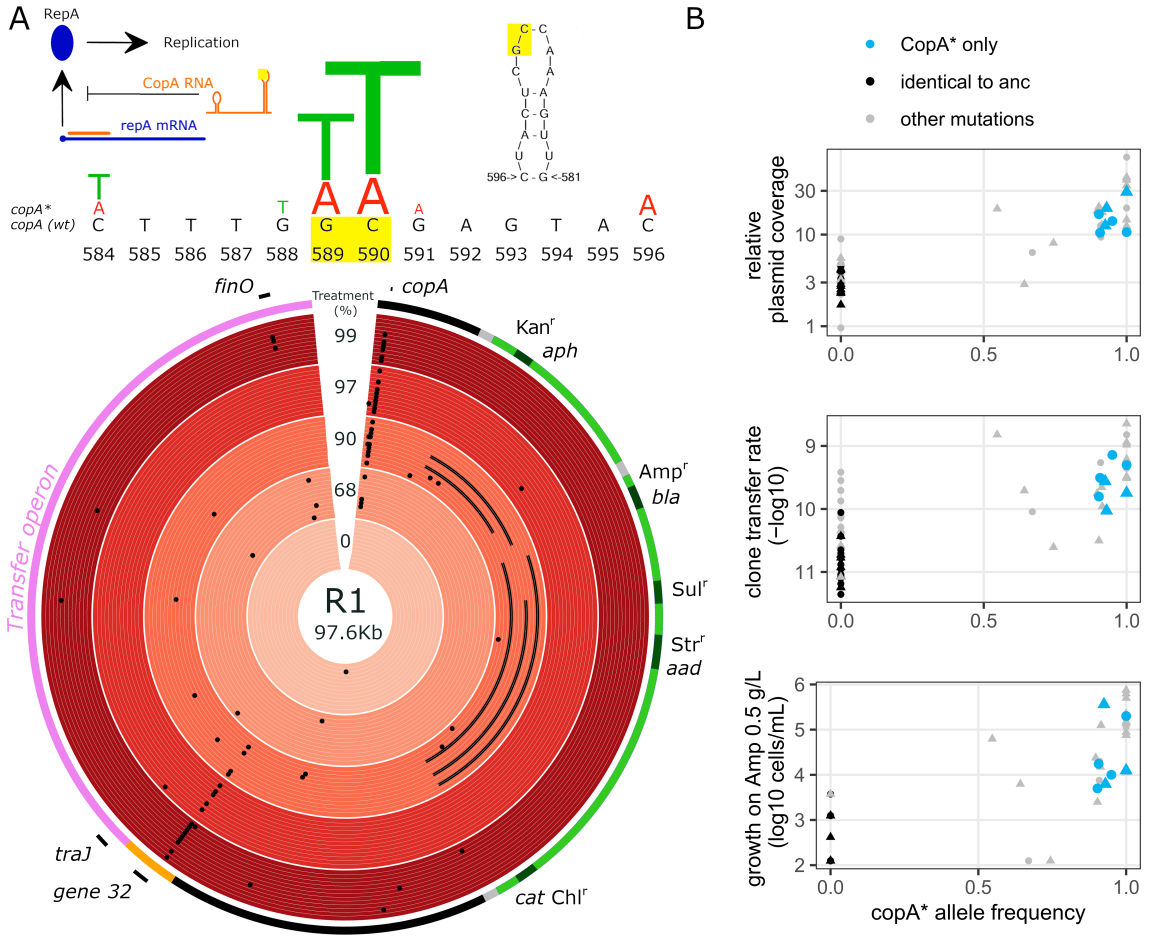

Figure 4: Molecular evolution and mechanistic basis for increased R1 transfer and AMR. A: Variants detected in evolved plasmids. The outermost ring of the circos plot shows a simplified plasmid map. Evolved plasmids are then shown by treatment, from outside in wt a-f then mut a-f clones. Black dots indicate small polymorphisms, lines show large deletions. Inset diagrams above show the secondary structure of CopA antisense RNA and its mode of action. Significant 13bp of evolved variants are summarised with letter size proportional to the relative abundance of each mutation. The position of the most common mutations in the second loop of CopA RNA is highlighted in yellow (modified from [24]). B: Phenotypic effects of *copA** variants. Evolved plasmid coverage, transfer rate and growth on Amp 0.5g/L are shown as a function of *copA** mutation frequency in the evolved clone (as not all plasmid copies necessarily have *copA** mutation). Blue dots indicate clones for which no other mutation than *copA** was present on the plasmid, and black dots indicate clones for which no mutation was detected on the plasmid.

An increase in R1 copy number couples transfer and AMR

Across all clones, only *copA** and *gene32* mutations were significantly associated with high transfer rates, *copA** having the strongest effect ($\log_{10}$ transfer rate ~ *copA**+ *gene32* + *finO*, *copA** effect 1.01±0.15, $F_{1,200}$=236, $p<2.10^{-16}$, *gene32* effect 0.30±0.16, $F_{1,200}$=12.0, p=0.0007). *finO* inactivation can strongly increase conjugation rate (see Figure 5A below), however no evolved plasmid carried *finO* mutations alone here, and its effect on transfer was non-significant (effect 0.22±0.27, F=2.4, p=0.12). Strikingly, seven evolved plasmids carried only a *copA** mutation and were otherwise identical to $R1_{wt}$ (blue dots in Figure 4B); these had on average a 17-fold increased transfer rate (*copA** effect, $F_{1,97}$=170, $p<2.10^{-16}$) in coevolved hosts, and 19-fold increased transfer rate when in the ancestral host (Figure S6, $F_{1,109}$=160, $p<2.10^{-16}$). *copA** variants also conferred a 55-fold increase in AMR on their hosts ($F_{1,25}$=45, $p=5.10^{-7}$), which is consistent with previous results on PCN effect on AMR [26–28]. Thus, *copA** mutations are sufficient to increase R1 transfer rate 17-fold and explain (via increased PCN) the increase in AMR. At high doses of other antibiotics to which R1 confers resistance (ampicillin, chloramphenicol and streptomycin), $R1_{copA*}$ also increased cell survival compared to $R1_{wt}$ and $R1_{finO}$ (Figure S7). Thus, increased gene dosage affects both the transfer region and other phenotypes encoded by R1.

To understand the mechanism by which transfer increases, we measured mobilisation of pMOB, a non-conjugative construct carrying R1 *oriT* (origin of transfer). pMOB can be mobilised by R1 transfer machinery, but its PCN is independently regulated, thus increases in pMOB transfer can only result from increased availability of R1 transfer machinery. A *finO* variant, which has derepressed expression of the transfer machinery[22] but no change in PCN, increased transfer of both itself and pMOB by around 1000-fold (Figure S8). A *copA** variant also increased transfer for both plasmids but mobilised pMOB ~4-fold less than itself ($R1_{CopA*}$ 26-fold, pMOB 6.5-fold, paired two-tailed t-test, p=0.0003). Thus, increased transfer of *copA** variants is due to the combination of increased transfer machinery expression (6.5-fold increased pMOB mobilisation), and increased number of copies of *oriT*. (4-fold R1-specific increase in mobilisation). Both effects are approximately of the same size than the 5-fold increase in PCN, suggesting they are due directly to increased gene dosage.

CopA variants spread better in the presence of immigration, despite their cost*

Finally, we characterised the fitness effects of a representative *copA** variant (w90d, carrying the unique mutation G589T) in competition with the ancestral plasmid (Figure 5A). In the absence of plasmid-free cells, $R1_{copA*}$ conferred a fitness cost to its host when competing with $R1_{wt}$. In the presence of 99% plasmid-free recipients, $R1_{copA*}$ instead had a selective advantage against $R1_{wt}$. This was due to horizontal transmission, as donor hosts containing $R1_{copA*}$ still decreased in frequency (Figure 5A, grey). Increased horizontal transmission also allowed *copA** variants to overcome the dilution caused by immigration, which $R1_{wt}$ was unable to do (Figure 5B). Thus, *copA** variants trade-off increased horizontal transmission against decreased vertical transmission, which is beneficial in conditions of high immigration. *finO* variants imposed a much higher cost to their hosts (Figure S9), which presumably limits the spread of *finO* variants relative to increased PCN.

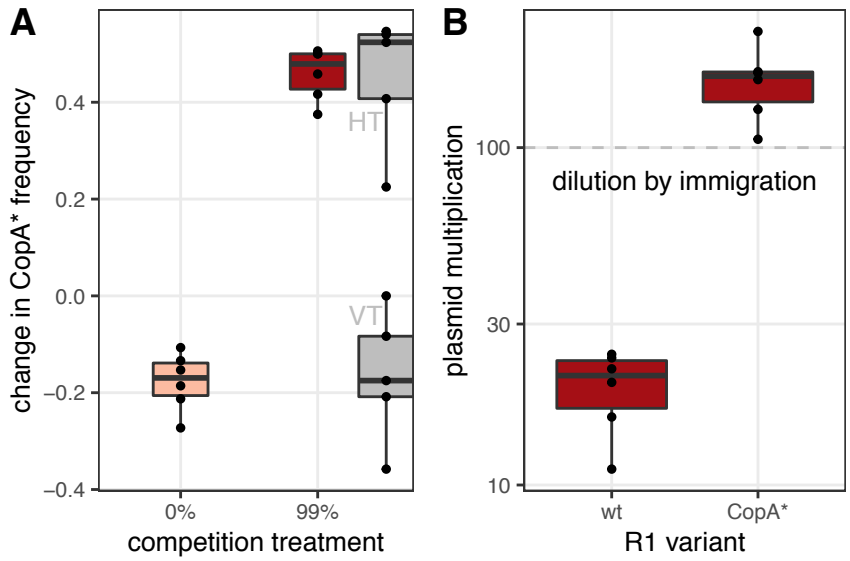

Figure 5: *copA variants trade-off vertical against horizontal transmission.** A: Change in frequency of $R1_{CopA*}$ in competition with $R1_{wt}$, in the absence or presence of immigration. In the presence of immigration (99% treatment), the change in frequency within initial donors (VT) and in transconjugants (HT) is shown in grey. The centre value of the boxplots shows the median, boxes show the first and third quartile, and whiskers represent 1.5 times the interquartile range; individual data points are shown as dots (N=6). B: Detail of the change in plasmid-carrying cell density for each variant in the presence of immigration. The centre value of the boxplots shows the median, boxes show the first and third quartile, and whiskers represent 1.5 times the interquartile range; individual data points are shown as dots.

Discussion

In the presence of susceptible hosts, we observed rapid evolution of increased horizontal transmission for R1, but not for RP4. Mutations able to increase transfer rate in RP4 might be constrained or too costly: regulation of transfer in RP4 makes increases in transfer expression hard to achieve [21], and increasing PCN, while possible, can be extremely costly[29]. For R1, despite a large increase in horizontal transmission with full derepression of the transfer operon, few clones evolved *finO* inactivation, likely because of its high cost to vertical transmission[30]. Instead, the most common mechanism for increased transfer was the evolution of increased PCN due to parallel mutations in CopA, which imposed some, but much lower, fitness costs. Similar PCN evolution could be common in other plasmids, as point mutations are frequently sufficient to change PCN, via changes in regulatory RNAs [25,26,31], or in Rep proteins [32,33]. Such changes likely always increase mobilisation in both conjugative and mobilisable plasmids, because of a direct increase in *oriT* dosage. For conjugative plasmids, increased gene dosage of the transfer operon might further increase transfer machinery activity, similarly to R1. Note however that, in contrast to our findings, high copy mutations in a conjugative IncI plasmid conferring colistin resistance were shown recently to negatively affect plasmid fitness despite an increase in horizontal transmission[34].

In addition to increased horizontal transmission, *copA** mutations also increased AMR through increased gene dosage. High levels of AMR correlated with high PCN have been observed previously [24,26–28]; we show here this can be driven by selection for transfer. Interestingly, specific coupling between horizontal transmission and AMR has been observed in other mobile elements [6,35], in which increased resistance gene expression also caused increased expression of transfer genes located immediately downstream. The effect we uncover here is more general, as all genes carried on the plasmid experience higher dosage. In R1, this translates into increased resistance at antibiotics concentrations not likely to be encountered naturally even under antibiotic treatment. However, similar increases in PCN might lead to clinically and environmentally relevant fitness benefits depending on plasmid accessory gene content. High PCN has been linked to increased resistance to low doses of antibiotics against which initial resistance is minimal [33,35–37]. Virulence and metabolic genes are also frequently carried on conjugative plasmids, and increased PCN has been linked to increased virulence in animal [38] and plant [39] pathogens, and to increased ability to grow on limiting nutrients[40].

Increased PCN could promote further evolution because multicopy plasmids have increased mutation supply[27]. Indeed, *copA** variants have significantly more additional SNPs than other evolved variants (Wilcoxon rank sum test, W=238, p=0.0009), suggesting that evolution of PCN is sufficient to rapidly increase evolvability. However, high PCN can also limit evolvability because any new mutation will be present on only one plasmid copy, affecting both genetic drift and selection[41]. Overall, PCN is a crucial component of plasmid life history, and modifying it can have far-reaching consequences through both gene dosage and evolvability[42].

Direct selection for cells containing conjugative plasmids usually removes plasmid-free hosts available for transfer, thus decreasing horizontal transmission overall [43]. We show here that selection for high gene dosage of plasmid-carried genes can, by contrast, favour highly transmissible plasmids, because of the pleiotropic effects of increased PCN. Another factor to consider in order to understand longer-term coevolution is the cost plasmid transmission imposes on hosts, and the resultant selection pressure. We observed here a few clones which evolved repression of plasmid transfer. Alternatively, selection for plasmid genes might favour alleles promoting transfer if plasmids are transferred to kin [44]. Increased horizontal transmission via high PCN creates a positive relationship between two traits central to plasmid life-history, coupling vertical and horizontal transmission components in ways that might complicate AMR management.

Methods

Strains, plasmids and growth conditions. The ancestral plasmid-bearing strains were *E. coli* MG1655 (wt) and MG1655 *mutL*::KnR (mut) obtained by transduction from the Keio collection [45]. Conjugative plasmids were R1 and RP4: R1 is an narrow-host-range IncFII plasmid, conferring resistance to Amp, kanamycin, sulphonamides, streptomycin and chloramphenicol. RP4 is a broad-host-range IncP plasmid conferring resistance to Amp, kanamycin and tetracycline. Plasmids were conjugated into ancestral strains from the MFDpir donor strain [19]. Plasmid-free immigrants were variants of wt and mut strains marked with *td-Cherry* [44] for transfers 1 to 15 and with a Δ*lac* deletion [46] for transfers 16 to 29; this allowed us to determine if plasmid-bearing clones were the original hosts, early or recent transconjugants,

by plating on XGal + IPTG and checking for red fluorescence. Cells were grown in LB medium, and plasmid-bearing clones were selected with Amp 100mg/L. Spontaneous rifampicin-resistant (Rif^R) and nalidixic acid-resistant (Nal^R) mutants of MG1655 [19] were used respectively as a standard donor host for measuring plasmid transfer from an ancestral genotype, and as a standard recipient in conjugation assays, using Rif 100 mg/L and Nal 30 mg/L for selection. Plasmids were transferred to plasmid-free backgrounds by conjugation, then transconjugants were selected on Amp + appropriate selection for the recipient phenotype. High-level evolved resistance to Amp was measured by plating on LB-agar + Amp 0.5g/L; when no colonies were detected a threshold value was calculated assuming one colony at the lowest dilution plated. Spontaneous mutants with increased antibiotic resistance using R1-carrying cells were obtained by plating 100 µL overnight cultures on Amp 500 mg/L + streptomycin (Str) 200 mg/L (as Amp alone was not sufficient to kill $R1_{wt}$-carrying cells at high cell density).

Evolution experiment and evolved clones. Evolving populations were grown in 200 µL LB medium in 96-well plates, at 37C with 180rpm shaking and 100-fold overall dilution every 24h, in the absence of any antibiotic. For immigration treatments, plasmid-free immigrants were grown fresh from glycerol stock and mixed with the evolving resident cultures in 99:1, 97:3, 90:10, 68:32 and 0:100 ratios at each passage. Plasmid-free *td-Cherry* strains were also passaged with 100-fold daily dilution. 6 replicate lineages were evolved per treatment x host strain (wt or mut) combination. One individual clone per lineage was picked for characterisation at 19 days (midpoint) and 29 days (endpoint) (Table S1). Plating and sequencing revealed a few instances of contamination between wells, detailed in Supplementary Text.

Conjugation assays. Plasmids-carrying donors and MG1655 Nal^R were grown overnight without antibiotic selection. Donor strains were first diluted 5-fold into LB medium and grown at 37C for 1h, then 20 µL diluted donor cultures were mixed with 20µL recipients and 160µL pre-warmed LB. After 1h mating, serial dilutions were plated on Amp, Nal and Amp+Nal to estimate densities of donors + transconjugants, recipients and transconjugants respectively. Conjugation rates were computed using the endpoint method[47], using 0.8 h^{-1} as the exponential growth rate (estimated independently from growth curves made with 100-fold dilution in LB). When no transconjugant was detected, a threshold conjugation rate was calculated by assuming that one single transconjugant colony was observed. The short 1h mating time was chosen in order to limit the effect of potential differences in growth rate or transfer rate between donors, recipients and transconjugants[48]. Replicates from ancestral host assays (Figure 1D y-axis,

Figure S3) with donor densities < 4.10^8 cells/mL and no transconjugants were discarded as they were found to correspond to a few wells in which strong evaporation occurred in the overnight donor culture prior to the conjugation assay.

Sequencing and bioinformatics. Clones selected for sequencing (Table S1) were grown overnight, with Amp selection for plasmid-carrying clones, and DNA was extracted using CTAB extraction. Illumina whole-genome sequencing was provided by MicrobesNG (http://www.microbesng.uk). Sequencing data were mapped to a reference genome combining MG151655 (GenBank accession NC_000913) and R1 plasmid (GenBank accession KY749247), using breseq 0.35.1 [49], run in polymorphism mode to account for the coexistence of several plasmid alleles in high PCN clones. Variants not present at frequency > 20% in at least one clone, and variants also detected in ancestral clones were discarded. Large deletions were called manually using coverage data, generated with breseq command bam2cov with default settings. Circos plots were made with R package omiccircos [50].

Mobilisation experiment. R1 *oriT* was amplified using primers 5'-CACGAAGCTTGCCTGCACTTTCGCCATATG-3' and 5'-CACCGAATTCAATCAGTGGCCTGGCAGATC-3', then cloned into pHERD30T plasmid [51], using restriction enzymes HindIII and EcoRI. The resulting plasmid pMOB was transformed into MG1655. pMOB-bearing cells were selected using 50 mg/L gentamycin (Gen), a dose necessary to avoid low-level resistance conferred by R1 variants. Clones containing both pMOB and a R1 variant were obtained by conjugation of R1 into MG1655 + pMOB using Amp+Gen selection. Mating was conducted as described above, but donor clone overnight cultures contained Amp+Gen, and mating time was reduced to 30min to limit secondary transfer; cells were also plated on Gen and Gen+Nal.

Plasmid fitness assays. After overnight growth without antibiotics, strains were mixed with equal ratios of plasmid-bearing competitors, and grown for 24h after 100-fold overall dilution in 96-well plates. Densities were estimated immediately after mixing and after 24h, by plating serial dilutions on selective medium. Competition assays in the absence of immigration were run using two-way competitions with *td-Cherry* and Δ*lac* marked MG1655 hosts , and plasmid variants were identified by the host background phenotype, as no transfer is taking place (N=6 for each combination, results with opposite host markers were pooled). Competition assays with immigration were run mixing 1% plasmid-carrying hosts with 99% MG1655 Nal^R.In this case, $R1_{CopA*}$ variants were distinguished from $R1_{wt}$ by streaking individual colonies on plates containing Amp 800mg/L and Strep 200mg/L (on which only $R1_{CopA*}$ clones are able to grow).

Antibiotics effects. Plasmid effect on survival in the presence of antibiotics was measured with plasmids carried by MG1655Δlac. Each strain was grown overnight in 8 independent replicates, without antibiotics, then dilution series were plated on agar with various concentrations of antibiotics. Survival was defined as colony-forming units (CFUs) on antibiotic medium / CFUs on LB agar without antibiotics. To survey growth in the presence of antibiotics for all evolved midpoint clones, cultures of evolved were first grown overnight in LB + Amp 100mg/L, then plated on agar with Amp 0.5 g/L.

Data analysis. Statistical analysis used R version 3.4.1 [52]. Transfer rate and cell density values were log-transformed before analysis. To analyse the effect of host background on clone transfer rate (Figure 2A), where data from each background were obtained in separate experiments, a bivariate model was run using the ASReml package with clone as a random effect [53].

Acknowledgments

We thank Alastair Wilson for help with statistical analysis. The work was funded by NERC (UK).

References

1. Frost, L. S., Leplae, R., Summers, A. O. & Toussaint, A. Mobile genetic elements: the agents of open source evolution. *Nature Reviews Microbiology* **3**, 722–732 (2005).
2. Lopatkin, A. J. *et al.* Persistence and reversal of plasmid-mediated antibiotic resistance. *Nature Communications* **8**, 1689 (2017).
3. van Hal, S. J., Wiklendt, A., Espedido, B., Ginn, A. & Iredell, J. R. Immediate Appearance of Plasmid-Mediated Resistance to Multiple Antibiotics upon Antibiotic Selection: an Argument for Systematic Resistance Epidemiology. *Journal of Clinical Microbiology* **47**, 2325–2327 (2009).
4. Baker, K. S. *et al.* Horizontal antimicrobial resistance transfer drives epidemics of multiple Shigella species. *Nature Communications* **9**, 1462 (2018).

5. Turner, P. E., Cooper, V. S. & Lenski, R. E. Tradeoff Between Horizontal and Vertical Modes of Transmission in Bacterial Plasmids. *Evolution* **52**, 315–329 (1998).
6. Turner, P. E. *et al.* Antibiotic resistance correlates with transmission in plasmid evolution. *Evolution* **68**, 3368–3380 (2014).
7. Smith, J. Superinfection drives virulence evolution in experimental populations of bacteria and plasmids. *Evolution* **65**, 831–841 (2011).
8. San Millan, A. & MacLean, R. C. Fitness Costs of Plasmids: a Limit to Plasmid Transmission. *Microbiology Spectrum* **5**, 0016 (2017).
9. San Millan, A. *et al.* Positive selection and compensatory adaptation interact to stabilize non-transmissible plasmids. *Nature Communications* **5**, 5208 (2014).
10. Harrison, E., Guymer, D., Spiers, A. J., Paterson, S. & Brockhurst, M. A. Parallel Compensatory Evolution Stabilizes Plasmids across the Parasitism-Mutualism Continuum. *Current Biology* **25**, 2034–2039 (2015).
11. Loftie-Eaton, W. *et al.* Compensatory mutations improve general permissiveness to antibiotic resistance plasmids. *Nature Ecology & Evolution* **1**, 1354–1363 (2017).
12. Anderson, R. M. & May, R. M. Coevolution of hosts and parasites. *Parasitology* **85**, 411–426 (1982).
13. Porse, A., Schønning, K., Munck, C. & Sommer, M. O. Survival and evolution of a large multidrug resistance plasmid in new clinical bacterial hosts. *Molecular Biology and Evolution* **33**, 2860–2873 (2016).
14. Dahlberg, C. & Chao, L. Amelioration of the cost of conjugative plasmid carriage in *Escherichia coli* K12. *Genetics* **165**, 1641–1649 (2003).

15. Dionisio, F., Conceição, I. C., Marques, A. C. R., Fernandes, L. & Gordo, I. The evolution of a conjugative plasmid and its ability to increase bacterial fitness. *Biology Letters* **1**, 250–252 (2005).

16. De Gelder, L., Williams, J. J., Ponciano, J. M., Sota, M. & Top, E. M. Adaptive Plasmid Evolution Results in Host-Range Expansion of a Broad-Host-Range Plasmid. *Genetics* **178**, 2179–2190 (2008).

17. Kottara, A., Hall, J. P. J., Harrison, E. & Brockhurst, M. A. Multi-host environments select for host-generalist conjugative plasmids. *BMC Evolutionary Biology* **16**, 70 (2016).

18. Messenger, S. L., Molineux, I. J. & Bull, J. J. Virulence evolution in a virus obeys a trade off. *Proceedings of the Royal Society B: Biological Sciences* **266**, 397–404 (1999).

19. Dimitriu, T., Marchant, L., Buckling, A. & Raymond, B. Bacteria from natural populations transfer plasmids mostly towards their kin. *Proceedings of the Royal Society B: Biological Sciences* **286**, 20191110 (2019).

20. Frost, L. S. & Koraimann, G. Regulation of bacterial conjugation: balancing opportunity with adversity. *Future Microbiology* **5**, 1057–1071 (2010).

21. Zatyka, M. & Thomas, C. M. Control of genes for conjugative transfer of plasmids and other mobile elements. *FEMS Microbiology Reviews* **21**, 291–319 (1998).

22. Yoshioka, Y., Ohtsubo, H. & Ohtsubo, E. Repressor gene finO in plasmids R100 and F: constitutive transfer of plasmid F is caused by insertion of IS3 into F finO. *Journal of bacteriology* **169**, 619–623 (1987).

23. Cox, K. E. L. & Schildbach, J. F. Sequence of the R1 plasmid and comparison to F and R100. *Plasmid* **91**, 53–60 (2017).

24. Nordström, K. Plasmid R1—Replication and its control. *Plasmid* **55**, 1–26 (2006).

25. Persson, C., Wagner, E. G. & Nordström, K. Control of replication of plasmid R1: structures and sequences of the antisense RNA, CopA, required for its binding to the target RNA, CopT. *The EMBO Journal* **9**, 3767–3775 (1990).

26. Santos-Lopez, A. *et al.* A naturally occurring SNP in plasmid pB1000 produces a reversible increase in antibiotic resistance. *Antimicrob. Agents Chemother.* **61**, e01735-16 (2016).

27. San Millan, A., Escudero, J. A., Gifford, D. R., Mazel, D. & MacLean, R. C. Multicopy plasmids potentiate the evolution of antibiotic resistance in bacteria. *Nature Ecology & Evolution* **1**, 0010 (2016).

28. Uhlin, B. E. & Nordström, K. R plasmid gene dosage effects in Escherichia coli K-12: copy mutants of the R plasmid R1drd-19. *Plasmid* **1**, 1–7 (1977).

29. Haugan, K., Karunakaran, P., Tøndervik, A. & Valla, S. The Host Range of RK2 Minimal Replicon Copy-Up Mutants Is Limited by Species-Specific Differences in the Maximum Tolerable Copy Number. *Plasmid* **33**, 27–39 (1995).

30. Haft, R. J. F., Mittler, J. E. & Traxler, B. Competition favours reduced cost of plasmids to host bacteria. *The ISME Journal* **3**, 761–769 (2009).

31. Muesing, M., Tamm, J., Shepard, H. M. & Polisky, B. A single base-pair alteration is responsible for the DNA overproduction phenotype of a plasmid copy-number mutant. *Cell* **24**, 235–242 (1981).

32. Thompson, M. G. *et al.* Isolation and characterization of novel mutations in the pSC101 origin that increase copy number. *Sci Rep* **8**, 1590 (2018).

33. Allen, R. C. & Brown, S. P. Modified Antibiotic Adjuvant Ratios Can Slow and Steer the Evolution of Resistance: Co-amoxiclav as a Case Study. *mBio* **10**, e01831-19, /mbio/10/5/mBio.01831-19.atom (2019).

34. Yang, J. *et al.* A ProQ/FinO family protein involved in plasmid copy number control favours fitness of bacteria carrying *mcr-1* -bearing IncI2 plasmids. *Nucleic Acids Research* **49**, 3981–3996 (2021).

35. Beabout, K. *et al.* Rampant Parasexuality Evolves in a Hospital Pathogen during Antibiotic Selection. *Molecular Biology and Evolution* **32**, 2585–2597 (2015).

36. Shen, Z. *et al.* Increased Plasmid Copy Number Contributes to the Elevated Carbapenem Resistance in OXA-232-Producing *Klebsiella pneumoniae*. *Microbial Drug Resistance* **26**, 561–568 (2020).

37. Rodriguez-Beltran, J. *et al.* Multicopy plasmids allow bacteria to escape from fitness trade-offs during evolutionary innovation. *Nature Ecology & Evolution* **2**, 873–881 (2018).

38. Wang, H. *et al.* Increased plasmid copy number is essential for Yersinia T3SS function and virulence. *Science* **353**, 492–495 (2016).

39. Cho, H. & Winans, S. C. VirA and VirG activate the Ti plasmid repABC operon, elevating plasmid copy number in response to wound-released chemical signals. *Proceedings of the National Academy of Sciences* **102**, 14843–14848 (2005).

40. Maisnier-Patin, S. & Roth, J. R. Selection and Plasmid Transfer Underlie Adaptive Mutation in *Escherichia coli*. *Genetics* **210**, 821–841 (2018).

41. Ilhan, J. *et al.* Segregational Drift and the Interplay between Plasmid Copy Number and Evolvability. *Molecular Biology and Evolution* **36**, 472–486 (2019).

42. Rodríguez-Beltrán, J., DelaFuente, J., León-Sampedro, R., MacLean, R. C. & San Millán, Á. Beyond horizontal gene transfer: the role of plasmids in bacterial evolution. *Nat Rev Microbiol* (2021) doi:10.1038/s41579-020-00497-1.

538 43. Hall, J. P. J., Williams, D., Paterson, S., Harrison, E. & Brockhurst, M. A. Positive
539 selection inhibits gene mobilization and transfer in soil bacterial communities. *Nature*
540 *Ecology & Evolution* **1**, 1348–1353 (2017).
541 44. Dimitriu, T. *et al.* Indirect Fitness Benefits Enable the Spread of Host Genes
542 Promoting Costly Transfer of Beneficial Plasmids. *PLoS Biology* **14**, e1002478 (2016).
543 45. Baba, T. *et al.* Construction of Escherichia coli K-12 in-frame, single-gene knockout
544 mutants: the Keio collection. *Molecular Systems Biology* **2**, 0008 (2006).
545 46. Dimitriu, T. *et al.* Negative frequency dependent selection on plasmid carriage and
546 low fitness costs maintain extended spectrum β-lactamases in Escherichia coli. *Scientific*
547 *Reports* **9**, 17211 (2019).
548 47. Simonsen, L., Gordon, D. M., Stewart, F. M. & Levin, B. R. Estimating the rate of
549 plasmid transfer: an end-point method. *Journal of general microbiology* **136**, 2319–2325
550 (1990).
551 48. Huisman, J. S. *et al.* Estimating the rate of plasmid transfer in liquid mating cultures.
552 22 (2020).
553 49. Deatherage, D. E. & Barrick, J. E. Identification of Mutations in Laboratory-Evolved
554 Microbes from Next-Generation Sequencing Data Using breseq. in *Engineering and*
555 *Analyzing Multicellular Systems* (eds. Sun, L. & Shou, W.) vol. 1151 165–188 (Springer
556 New York, 2014).
557 50. Hu, Y. *et al.* OmicCircos: A Simple-to-Use R Package for the Circular Visualization of
558 Multidimensional Omics Data. *Cancer Inform* **13**, CIN.S13495 (2014).
559 51. Qiu, D., Damron, F. H., Mima, T., Schweizer, H. P. & Yu, H. D. PBAD-Based Shuttle
560 Vectors for Functional Analysis of Toxic and Highly Regulated Genes in Pseudomonas and

561 Burkholderia spp. and Other Bacteria. *Applied and Environmental Microbiology* **74**, 7422–
562 7426 (2008).
563 52. R Development Core Team. R: A language and environment for statistical computing.
564 R Foundation for Statistical Computing,. *Vienna, Austria. ISBN 3-900051-07-0, URL*
565 *http://www.R-project.org.* (2008).
566 53. Houslay, T. M. & Wilson, A. J. Avoiding the misuse of BLUP in behavioural ecology.
567 *Behavioral Ecology* **28**, 948–952 (2017).
568
569

Supplementary text

Evidence for contamination during the evolution experiment

The evolution experiment was carried out using 96-well culture plates, which is associated with a higher risk for cross-contamination. We detected evidence of some contamination, based on molecular markers of ancestral / immigrant strains, and on whole-genome sequencing results, both described below:

- The experiment was designed with initial plasmid hosts being "blue" (no red fluorescence, and presence of the active lac operon, leading to blue colonies when plating on XGal+IPTG), early immigrants being red, and late immigrants being "white" (lac deletion leading to white colonies when plating on XGal+IPTG). The 'no immigration' or 0% treatment was founded with only initial plasmid hosts, thus should have contained only blue cells. However, from passage 16, all 6 mut lineages contained some red clones, with 3 of 6 lineages having only red clones. This might be due to cross-contamination between wells, or (most likely in our opinion) a pipetting mistake that introduced once some red immigrants to all 6 wells.
- Plasmid-free controls were run in parallel to the plasmid evolution treatments, on the same 96-well plate. One out of twelve sequenced "plasmid-free" hosts resulted in plasmid reads, mapping to R1 but with the loss of the whole antibiotic resistance region (shown in Figure S5), a definitive evidence for cross-well contamination.

Genomic analysis and variants of interest

- *Manual inspection of plasmid mutation data:*

Breseq was run in polymorphism mode to account for the presence of high copy number variants, and cases in which mutations were not present on all plasmid copies. In order to exclude sequencing errors, we then excluded mutations that were present in <20% frequency in all samples. Two other types of variants were excluded:

i) The mutation 58157 C>T was present in all samples, including the ancestral plasmids, and represents a divergence from the published sequence.

ii) We observed a cluster of complex mutations positions 87616-87664, within the coding sequence of *traD*, in the ancestor and many (but not all) of the evolved plasmid sequences. They were all insertions or deletions of 9 nucleotides, leading to amino-acid changes but no frameshift or stop codon. A similar 9bp insertion is also found in AY684127 accession of R1 *traD* sequence, suggesting it is not specific to this evolution experiment. Thus, all variants at these positions were excluded from the analysis.

Large deletions were also added manually, after analysis of coverage plots. Four large deletions were detected on evolved R1 plasmids:

Clone	Genome coordinates of deletions
W90b	18390 to 40664
W90e	6200 to 17100
	22124 to 40664
M90b	6200 to 15335
M90c	18289 to 40664

In addition, coverage plots (Figure S6) show changes in coverage that suggest coexistence of plasmids with full and deleted genomes, with changes in coverage corresponding to the location of insertion sequences on R1 genome.

- *Variants of interest:*

Mutations suggesting parallel evolution are described in the main text. In addition, here we present more detailed information on other variants that might have phenotypic effects on R1 transfer rate.

Three mutations were detected in or close to the *traJ* gene. Clones m99a and w90f each had a point mutation respectively 49bp and 30bp before the start of the coding sequence; clone w97a had a point mutation within the coding sequence, leading to a change in protein sequence (K42E).

The clone mut68d carried a point mutation from A to G at position 83395, within the coding sequence of *traG*, leading to an amino-acid change, Q663R in protein TraG. TraG is involved in mating pair stabilisation, but also entry exclusion (1): when a plasmid is present in the recipient cell, it expresses TraS entry exclusion protein at its surface, and TraG -TraS interaction decreases transfer rate by 1000-fold. In F plasmid, the specific recognition of TraS was shown to be due to the region between aa 610 and 673, and plasmid R100 TraG, which differs from F TraG only in this same region, does not cause entry exclusion from F (1). This suggests that mutation Q663R might allow the evolved mut68d variant to avoid entry exclusion from the wildtype R1 plasmid, similarly to what has been observed with a variant of R1 previously (2).

Finally, we sequenced an additional clone, m68e-t12. We first noticed that R1 plasmid from clone m68e isolated after 19 days of evolution has high transfer rate when present in the ancestor *E. coli* host but not when in its coevolved clone (Figure 1D), suggesting that the coevolved host repressed transfer. Thus, we analysed a clone from the same lineage but isolated earlier, hoping that we might obtain the same plasmid variant but different regulation by the host. Instead, m68e-t12 plasmid carries only one single mutation within the *finO* gene, similar to the ones described in the main text for other evolved variants. We used this *finO* variant in phenotypic and fitness assays as a example of derepression of transfer, as midpoint evolved *finO* clones (Figure 4A) all carry other mutations as well.

References

1. Audette GF, Manchak J, Beatty P, Klimke WA, Frost LS. Entry exclusion in F-like plasmids requires intact TraG in the donor that recognizes its cognate TraS in the recipient. Microbiology. 2007;153(2):442–51.

2. Smith J. Superinfection drives virulence evolution in experimental populations of bacteria and plasmids. Evolution. 2011;65(3):831–41.

Evolution of plasmid conjugation rates: detailed analysis and statistical tests

We examined the effect of two factors in the evolution of plasmid conjugation rates: immigration treatment, and host background (wt or mut). As seen below, immigration treatment had the strongest effect on evolved conjugation rates, but the interaction between immigration treatment and host background was significant, mut hosts being associated to the evolution of higher transfer rates particularly for high immigration treatments. Evolution in high immigration treatments might be the most dependent on high mutation rates because plasmid-bearing lineages will be subject to strong bottlenecks limiting genetic diversity.
We also present below the results of models including only immigration treatment, from which the statistical values presented in the main text are taken.

- Conjugation from coevolved donor hosts:

Model: lm($\log_{10}$ transfer rate~strain*treatment)

	Df	Sum Sq	Mean Sq	F value	Pr(>F)	
strain	1	0.64	0.643	2.537	0.112831	
treatment	5	59.55	11.911	47.013	< 2e-16	***
strain:treatment	5	5.47	1.094	4.319	0.000955	***
Residuals	192	48.64	0.253			

Coefficients:

	Estimate	Std. Error	t value	Pr(>|t|)	
(Intercept)	-10.64945	0.14530	-73.292	< 2e-16	***
Strain mut	-0.07987	0.20549	-0.389	0.697935	
treatment 99%	0.61097	0.18758	3.257	0.001331	**
treatment 97%	0.73612	0.18758	3.924	0.000121	***
treatment 90%	1.33969	0.18758	7.142	1.85e-11	***
treatment 68%	0.11721	0.18758	0.625	0.532802	
treatment 0%	-0.35686	0.18758	-1.902	0.058616	.
strainmut:treatment 99%	0.60526	0.26528	2.282	0.023612	*
strainmut:treatment 97%	0.47830	0.26528	1.803	0.072960	.
strainmut:treatment 90%	-0.38143	0.26528	-1.438	0.152113	
strainmut:treatment 68%	0.22230	0.26528	0.838	0.403088	
strainmut:treatment 0%	0.16436	0.26528	0.620	0.536269	

Model: lm($\log_{10}$ transfer rate~treatment)

	Df	Sum Sq	Mean Sq	F value	Pr(>F)	
treatment	5	59.55	11.911	43.07	<2e-16	***
Residuals	198	54.76	0.277			

Coefficients:

	Estimate	Std. Error	t value	Pr(>|t|)	
(Intercept)	-10.6894	0.1073	-99.581	< 2e-16	***
Treatment 99%	0.9136	0.1386	6.593	3.84e-10	***
Treatment 97%	0.9753	0.1386	7.038	3.13e-11	***
Treatment 90%	1.1490	0.1386	8.291	1.69e-14	***
Treatment 68%	0.2284	0.1386	1.648	0.1010	
Treatment 0%	-0.2747	0.1386	-1.982	0.0489	*

- Conjugation of evolved plasmids from unevolved standard host:

Model: lm(log_{10} transfer rate~strain*treatment)

```
                  Df Sum Sq Mean Sq F value   Pr(>F)
strain             1  11.75  11.747  23.964 1.94e-06 ***
treatment          5  56.85  11.371  23.197  < 2e-16 ***
strain:treatment   5  12.66   2.533   5.167  0.00017 ***
Residuals        212 103.92   0.490
```

```
Coefficients:
                           Estimate Std. Error t value Pr(>|t|)
(Intercept)                -11.42673    0.18077 -63.211  < 2e-16 ***
strainmut                   -0.04456    0.25565  -0.174  0.86179
treatment 99%                0.27577    0.23669   1.165  0.24527
treatment 97%                0.79269    0.24182   3.278  0.00122 **
treatment 90%                1.34303    0.24182   5.554 8.32e-08 ***
treatment 68%                0.47300    0.24477   1.932  0.05464 .
treatment 0%                -0.05751    0.24477  -0.235  0.81448
strainmut:treatment 99%      1.24338    0.33473   3.715  0.00026 ***
strainmut:treatment 97%      0.63664    0.34408   1.850  0.06566 .
strainmut:treatment 90%     -0.01676    0.34408  -0.049  0.96119
strainmut:treatment 68%      0.80598    0.33617   2.398  0.01737 *
strainmut:treatment 0%       0.10797    0.34615   0.312  0.75542
```

Model: lm(log_{10} transfer rate~treatment)

```
             Df Sum Sq Mean Sq F value   Pr(>F)
treatment     5  56.88  11.377   19.33 6.49e-16 ***
Residuals   218 128.30   0.589
```

```
Coefficients:
               Estimate Std. Error t value Pr(>|t|)
(Intercept)   -11.449013   0.140062 -81.742  < 2e-16 ***
Treatment 99%   0.897462   0.183384   4.894 1.92e-06 ***
Treatment 97%   1.103006   0.188477   5.852 1.76e-08 ***
Treatment 90%   1.335483   0.188477   7.086 1.89e-11 ***
Treatment 68%   0.930379   0.183384   5.073 8.35e-07 ***
Treatment 0%   -0.003522   0.189645  -0.019    0.985
```

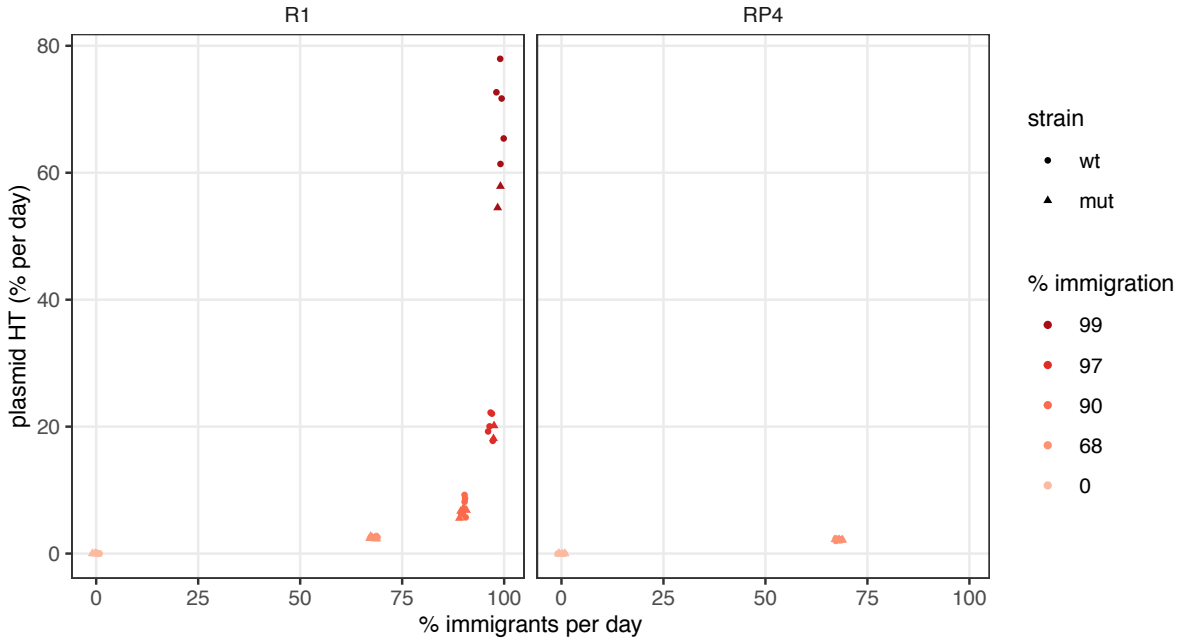

Figure S1: Average horizontal transmission per day. Theoretical plasmid-bearing cell proportions with only vertical transmission, $pred_{19}$, were calculated after 19 days assuming equal fitness for all hosts ($pred_{19} = (1 - \%immigration)^{19}$). Plasmid spread by horizontal transmission (HT) was defined as the average daily increase in plasmid-bearing cell proportion necessary to explain observed plasmid-bearing cell proportions at day 19 ($obs_{19} = (1 - \%immigration + HT)^{19}$). Thus, HT per day is calculated as $HT = \left(1 - \%\frac{immigration}{100}\right) * \left(1 + \sqrt[19]{\frac{obs_{19}}{pred_{19}}}\right)$.

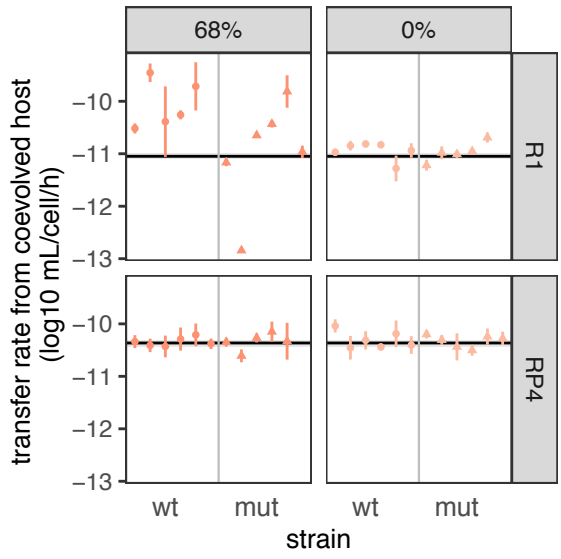

Figure S2: Endpoint (29 days) plasmid conjugation rates. The black line and shaded area are respectively the geometric mean and standard error (SE) of ancestral plasmid transfer rate; each coloured dot and line indicates respectively the geometric mean and SE of evolved clones (N=3).

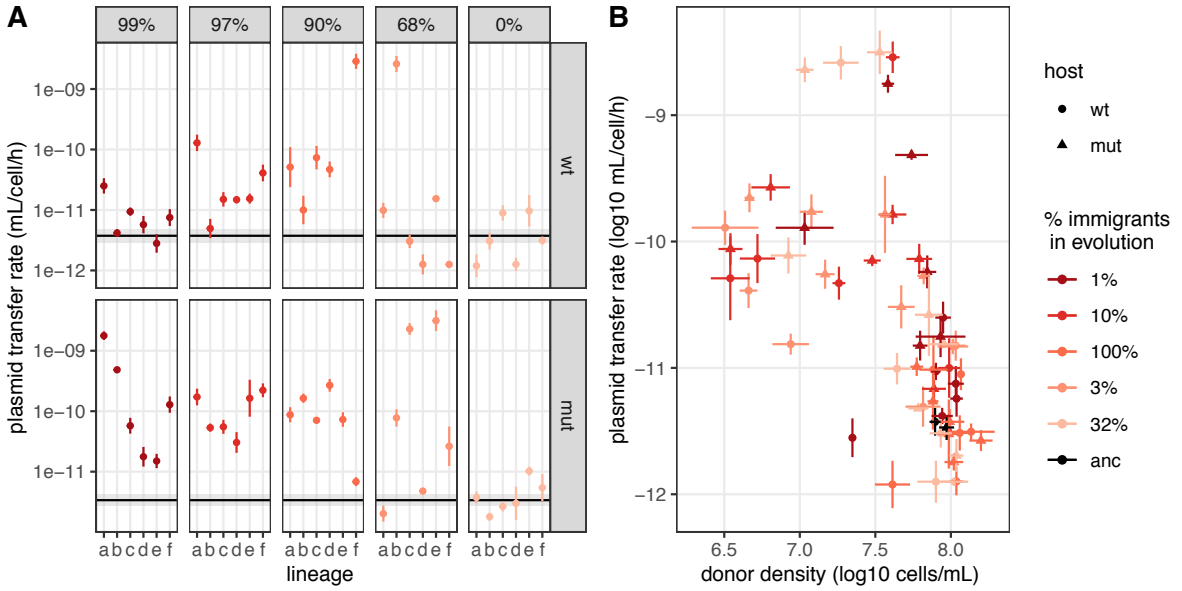

Figure S3: Midpoint R1 plasmid specific conjugation rates (A) and associated trade-off with donor density (B). Plasmid transfer rates were measured from plasmid-bearing ancestral hosts towards the standard recipient strain MG1655 Nal^R. Dots are geometric averages and lines indicate geometric standard errors (N=3). In A, the black line and shaded area are respectively the geometric average and standard error of ancestral plasmid transfer rate. In B, transfer rates measured from ancestral hosts are shown as a function of donor host cell density at the end of the conjugation assay. Statistics are described in Supplementary Text.

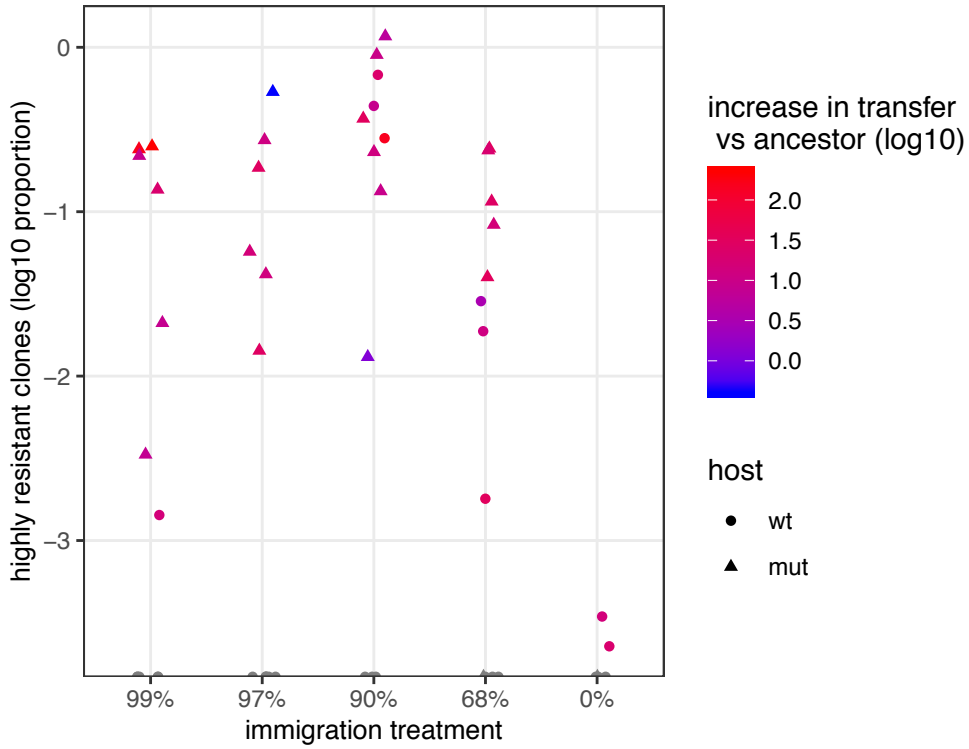

Figure S4: Proportion of highly resistant plasmids after selection for transfer. The proportion of plasmid-bearing cells able to grow in the presence of 0.5g/L Amp is shown as a function of immigration treatment in 9 day evolved populations. For each population, a clone was picked randomly, and its transfer rate was measured (N=2). Dot colour indicates the ration of evolved transfer rate to ancestral R1 transfer rate ($\log_{10}$).

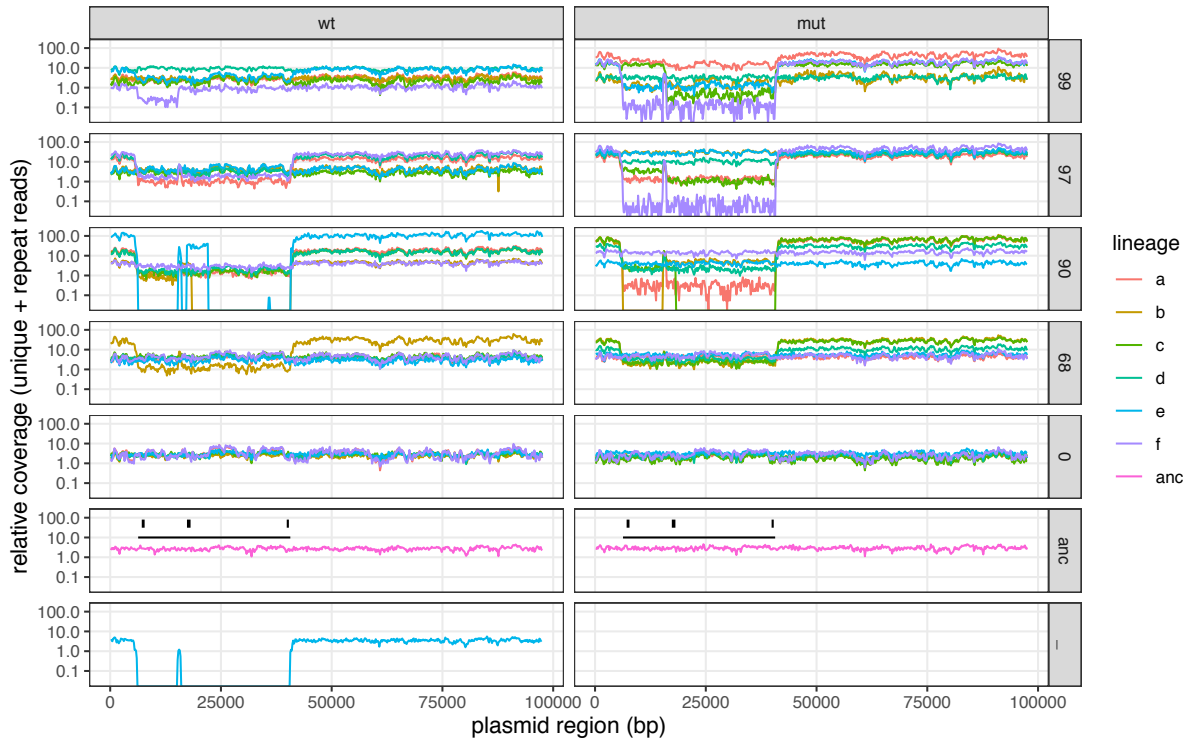

Figure S5: Variation in sequencing coverage across R1 plasmid map. Relative coverage of sequencing reads is shown for all clones across $R1_{wt}$ sequence map. Relative coverage was measured as the sum of coverage of both unique and repeat reads, divided by the overall average coverage of reads mapped to the chromosome. Black rectangles above the ancestor graph indicate the position of genes conferring antibiotic resistance (from left to right: kanamycin, ampicillin and chloramphenicol), and the black line indicates the whole resistance determinant region (bordered by insertion sequences). In the plasmid-free control treatment (bottom), reads mapping to the plasmid were detected for lineage w_e, indicating contamination by a plasmid missing the whole resistance determinant. All other clones retained at least the *bla* gene conferring Amp resistance, as they were obtained by plating on Amp-containing medium.

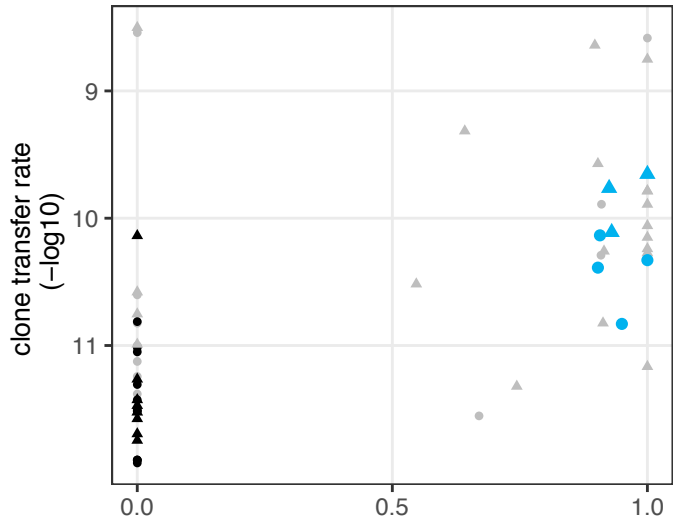

Figure S6: Effect of *copA variants on evolved plasmid transfer rate from the ancestral host.** Evolved rate is shown as a function of *copA** mutation frequency in the evolved clone. Black dots indicate clones for which no mutation was detected on the plasmid; blue dots clones for which no other mutation than *copA** was present on the plasmid.

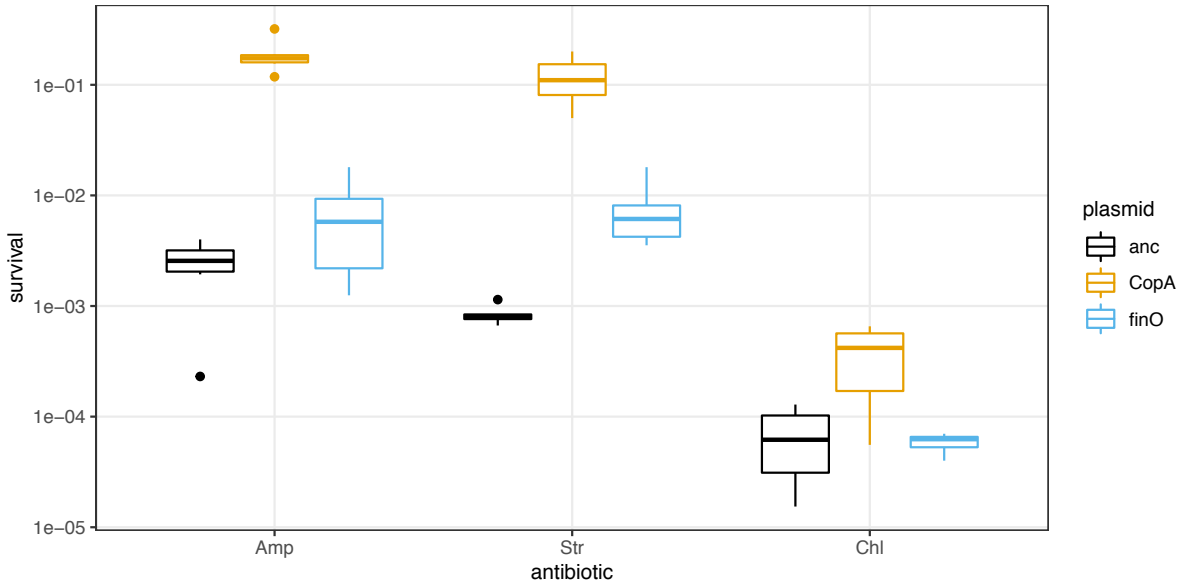

Figure S7: Effect of antibiotics on cells carrying R1 variants. Survival in the presence of high doses of antibiotics to which R1 carries resistance determinants. Antibiotics tested were ampicillin 500 mg/L (Amp), streptomycin 200 mg/L (Str) and chloramphenicol 600 mg/L (Chl); R1 carries resistance determinants to the three last antibiotics. Dots indicate individual populations; the centre value of the boxplots is the median and boxes denote the interquartile range (*N=8*).

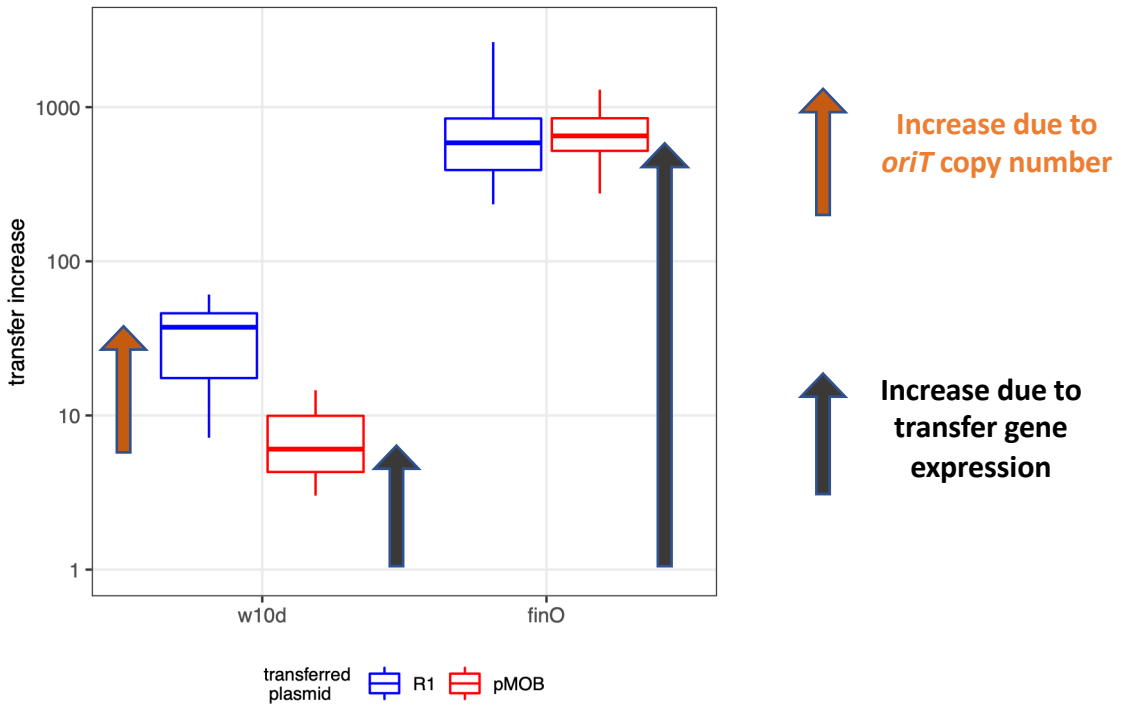

Figure S8: Impact of evolved *copA variants on plasmid mobilisation *in trans*.** R1 transfer was measured together with mobilisation of pMOB carrying R1 *oriT*. Increased transfer operon expression will increase transfer of both plasmids, whereas increased *oriT* copy number will only increase R1 transfer. The increase in transfer compared to $R1_{wt}$ is shown for each R1 variant and associated pMOB plasmid. The centre value of the boxplots shows the median, boxes the first and third quartile, and whiskers represent 1.5 times the interquartile range ($N=8$).

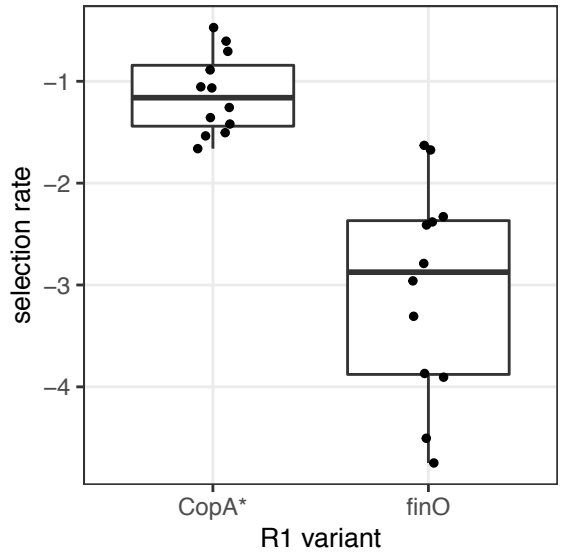

Figure S9: selection rate of CopA* and finO variants in competition against R1wt, in the absence of plasmid-free immigrants. The centre value of the boxplots shows the median, boxes show the first and third quartile, and whiskers represent 1.5 times the interquartile range; individual data points are shown as dots.

Table S1: Detail of characterized R1 clones. Midpoint clones were isolated between passage 16 and passage 19: one Amp resistant clone per lineage was chosen randomly for each lineage. When possible, clones from passage 19 were isolated but in lineages where plasmid-bearing cells were already extinct at passage 19, one clone was isolated from populations from passages 17 or 16. Two additional clones from the m68e lineage were isolated from different timepoints and sequenced; the m68e_t12 clone was found to carry only one mutation in *finO* (see Dataset S1).

Dataset S1: Sequence variants detected in evolved clones. A table was generated with breseq option gdtools COMPARE, then manually cleaned. For the plasmid, two types of mutations were discarded. One was a point mutation 58157 C>T, present in the ancestor and all evolved plasmids. The second was a cluster of complex mutations in positions 87616-87664, within *traD* CDS (see details in Supplementary Text). For the chromosome, variants with less than 100% allele frequency were discarded.

Table S1: Detail of characterized R1 clones. Midpoint clones were isolated between passage 16 and passage 19: one Amp resistant clone per lineage was chosen randomly for each lineage. When possible, clones from passage 19 were isolated but in lineages where plasmid-bearing cells were already extinct at passage 19, one clone was isolated from populations from passages 17 or 16. Two additional clones from the m68e lineage were isolated from different timepoints and sequenced; the m68e_t12 clone was found to carry only one mutation in *finO* (see Dataset S1).

clone name	background	plasmid	immigration	lineage	day clone isolation	day last detected	marker
wt_R1	mut	R1	ancestor	ancestor			blue (lac+)
mut_R1	mut	R1	ancestor	ancestor			blue (lac+)
MGred	wt	/	ancestor	ancestor			red (td-Cherry)
MGΔlac	wt	/	ancestor	ancestor			white (Δlac)
m68e_t12	mut	R1	68%	e	12		red
m68e_t29	mut	R1	68%	e	29		white
w99_a	wt	R1	99%	a	19	19	white
w99_b	wt	R1	99%	b	19	19	white
w99_c	wt	R1	99%	c	19	19	white
w99_d	wt	R1	99%	d	19	19	white
w99_e	wt	R1	99%	e	17	17	white
w99_f	wt	R1	99%	f	19	25	white
m99_a	mut	R1	99%	a	19	19	white
m99_b	mut	R1	99%	b	17	17	white
m99_c	mut	R1	99%	c	16	16	red
m99_d	mut	R1	99%	d	17	17	white
m99_e	mut	R1	99%	e	19	19	white
m99_f	mut	R1	99%	f	16	16	red
w97_a	wt	R1	97%	a	19	19	white
w97_b	wt	R1	97%	b	17	17	white
w97_c	wt	R1	97%	c	19	25	white
w97_d	wt	R1	97%	d	19	19	white
w97_e	wt	R1	97%	e	19	19	white
w97_f	wt	R1	97%	f	19	19	white
m97_a	mut	R1	97%	a	19	19	white
m97_b	mut	R1	97%	b	19	19	red
m97_c	mut	R1	97%	c	17	17	white
m97_d	mut	R1	97%	d	16	16	red
m97_e	mut	R1	97%	e	17	17	white

m97_f	mut	R1	97%	f	17	17	white
w90_a	wt	R1	90%	a	19	25	white
w90_b	wt	R1	90%	b	19	29	white
w90_c	wt	R1	90%	c	19	19	red
w90_d	wt	R1	90%	d	19	19	white
w90_e	wt	R1	90%	e	19	25	white
w90_f	wt	R1	90%	f	19	29	red
m90_a	mut	R1	90%	a	17	17	white
m90_b	mut	R1	90%	b	19	19	white
m90_c	mut	R1	90%	c	19	19	white
m90_d	mut	R1	90%	d	19	19	red
m90_e	mut	R1	90%	e	19	25	red
m90_f	mut	R1	90%	f	19	19	red
w68_a	wt	R1	68%	a	19	29	blue
w68_b	wt	R1	68%	b	19	29	red
w68_c	wt	R1	68%	c	19	29	blue
w68_d	wt	R1	68%	d	19	29	red
w68_e	wt	R1	68%	e	19	29	blue
w68_f	wt	R1	68%	f	19	29	red
m68_a	mut	R1	68%	a	19	29	red
m68_b	mut	R1	68%	b	19	29	red
m68_c	mut	R1	68%	c	19	29	red
m68_d	mut	R1	68%	d	19	29	red
m68_e	mut	R1	68%	e	19	29	red
m68_f	mut	R1	68%	f	19	29	red
w0_a	wt	R1	0%	a	19	29	blue
w0_b	wt	R1	0%	b	19	29	blue
w0_c	wt	R1	0%	c	19	29	blue
w0_d	wt	R1	0%	d	19	29	blue
w0_e	wt	R1	0%	e	19	29	blue
w0_f	wt	R1	0%	f	19	29	blue
m0_a	mut	R1	0%	a	19	29	red
m0_b	mut	R1	0%	b	19	29	blue
m0_c	mut	R1	0%	c	19	29	red
m0_d	mut	R1	0%	d	19	29	blue
m0_e	mut	R1	0%	e	19	29	red
m0_f	mut	R1	0%	f	19	29	blue